



**Search for the Higgs boson in $H \rightarrow WW^* \rightarrow ee$ decays
with 0.63 fb^{-1} at DØ in Run IIb**

The DØ Collaboration

(Dated: September 29, 2007)

A search for the Higgs boson is presented in $H \rightarrow WW^* \rightarrow ee$ decays in $p\bar{p}$ collisions at a center-of-mass energy of $\sqrt{s} = 1.96 \text{ TeV}$. Final states containing two electrons have been considered. The data, corresponding to an integrated luminosity of about $\sim 630 \text{ pb}^{-1}$, has been collected from June 2006 to July 2007 using the Run IIb DØ detector. No significant excess above the Standard Model background has been observed, and limits on the cross section for $m_H = 120, 140, 160, 180$ and 200 GeV have been set.

Preliminary Results for P5 Meeting

I. INTRODUCTION

In this note a search for the Higgs boson decaying into the WW^* final state with the D0 detector at the Tevatron collider at $\sqrt{s} = 1.96$ TeV at Fermilab is presented. Leptonic decay modes $H \rightarrow WW^* \rightarrow ee$ are considered, leading to final states with two electrons and missing transverse momentum. The $H \rightarrow WW^* \rightarrow \ell\ell$ decay mode provides the largest sensitivity for the Standard Model Higgs boson search at the Tevatron with a mass of $m_H \sim 160$ GeV [1–3]. Additionally the Higgs boson masses $m_H \sim 120, 140, 160$ and 200 GeV have been analyzed. The present analysis taking advantage of the ee final state is complementary to the $H \rightarrow WW^* \rightarrow \ell\ell' (\ell, \ell' = e, \mu)$ analysis presented in [4]. When combined with searches exploiting the WH and ZH associated production, this decay mode increases the sensitivity for Higgs boson searches.

II. DATA AND MC SAMPLES

The data sample used in this analysis has been collected between June 2006 and April 2007 by the D0 detector at the Fermilab Tevatron Collider. The NNLO $Z/\gamma^* \rightarrow ee$ cross section has been scaled to the data in the mass region $80 \text{ GeV} < M_{ee} < 110 \text{ GeV}$. The events are selected using various single and di-electron triggers. Applying this normalization leads to a total luminosity \times trigger efficiency of $\sim 630 \text{ pb}^{-1}$. The total luminosity recorded during RunII is about 1700 pb^{-1} from which this analysis covers the most recent run period. DATA to Monte Carlo(MC) correction factors have been applied to MC before normalization to $Z/\gamma^* \rightarrow ee$. The systematic uncertainties on the normalization factor include the $Z/\gamma^* \rightarrow ll$ cross section, the PDF uncertainty and the statistical uncertainty on the data/Monte Carlo normalization factor. As the MC is normalized to data, luminosity blocks marked as "bad" by the luminosity system are retained.

Signal and Standard Model background processes have been generated with the PYTHIA 6.319 [5] Monte Carlo (MC) generator using the CTEQ6L1 parton distribution functions and subsequent use of GEANT which provides a detailed simulation of the detector geometry. MC events are then processed further with the same reconstruction software as used for data. All background processes, apart from QCD multijet production, are normalized using cross sections calculated at next-to-leading order (NLO) or next-to-next-to-leading order (NNLO) based on the parton distribution functions. The signal cross sections have been calculated at NNLO, using HDECAY [6]. The expected signal for all Higgs masses is given in Table. III. The background contribution from QCD multijet production where jets are misidentified as leptons is estimated from the data itself by using like-sign ee events which were selected by inverting lepton identification and calorimeter isolation criteria. The samples are normalized to the data as function of p_T at an early stage of the selection in a region of phase space dominated by multijet production.

The $Z/\gamma \rightarrow ll$ cross section is calculated with CTEQ6L1 PDFs as $\sigma(Z/\gamma \rightarrow ll) = \sigma_{LO} \times K_{QCD}(Q^2)$, with the LO cross section calculated by Pythia LO PDF and the K_{QCD} at NNLO with NLO PDF, calculated according to [7, 8]. The $W \rightarrow e\nu$ cross section is calculated with NNLO corrections and PDFs. The $t\bar{t}$ cross section is calculated at NNLO in [9] and the WW, ZZ and WZ cross sections are calculated with MCFM v3.4.5 CTEQ5L for LO and CTEQ5M (for NLO). The uncertainties due to the PDF uncertainty is calculated in [8].

III. EVENT SELECTION

Electrons are identified by using calorimeter and tracking information. Electromagnetic showers are identified in the calorimeter, these showers are chosen by comparing the longitudinal and transverse shower profiles to those of simulated electrons. The showers must be isolated, deposit most of their energy in the electromagnetic part of the calorimeter and pass a likelihood criterion that includes a spatial track match and, in the central detector region, an E/p requirement, where E is the energy of the calorimeter cluster and p is the momentum of the track. Both electrons must stem from the primary vertex and be reconstructed within a detector pseudorapidity $|\eta| < 3.0$. The transverse momentum measurement of the electrons is based on calorimeter cell energy information. The decay of the two W bosons results in three different final states $e^+e^- + X$ (ee channel), $e^\pm\mu^\mp + X$ ($e\mu$ channel) and $\mu^+\mu^- + X$ ($\mu\mu$ channel), each of which consist of two oppositely charged isolated high transverse momentum leptons and large missing transverse energy \cancel{E}_T due to escaping neutrinos. The event kinematics change significantly as function of the Higgs mass. The mass dependent selection procedure is summarized in Table I. It will be justified and described more detailed in the following.

The signal is characterized by two leptons, missing transverse momentum and little jet activity. The selection for the ee channel as presented in this analysis requires two oppositely charged leptons with $p_T > 20$ GeV for the leading electron and $p_T > 15$ GeV for the trailing electron. Additionally the di-lepton mass is required to exceed 15 GeV. Figure 1a shows the invariant dilepton mass distribution in data, background and signal at this stage of the

Selection criteria	$m_H = 120$	$m_H = 140$	$m_H = 160$	$m_H = 180$	$m_H = 200$
Cut 0 Preselection	lepton ID, leptons with opposite charge, $m_{ee} > 15$ GeV and $p_T^{e1} > 20$ GeV and $p_T^{e2} > 15$ GeV both leptons not matched				
Cut 1 Invariant mass M_{ee}	< 60	< 70	< 80	< 80	< 80
Cut 2 Missing Transverse Energy \cancel{E}_T	> 20	> 20	> 20	> 20	> 20
Cut 3 $\cancel{E}_T^{\text{Scaled}}$	> 7	> 7	> 7	> 7	> 7
Cut 4 $M_{min}^T(l, \cancel{E}_T)$	> 40	> 45	> 55	> 60	> 65
Cut 5 Sum of $p_T^l + p_T^{l'} + \cancel{E}_T$	90-140	100-160	110-180	110-180	120-200
Cut 6 H_T	< 100	< 100	< 100	< 100	< 100

TABLE I: Summary of the selection criteria for the various Higgs masses $m_H = 120$ GeV, $m_H = 120$ GeV, $m_H = 140$ GeV, $m_H = 160$ GeV, $m_H = 180$ GeV and $m_H = 200$ GeV.

selection. This stage is referred to as preselection stage. Most of the $Z \rightarrow \ell\ell$ events are rejected by requiring an upper limit for the invariant dielectron mass which is listened for the various Higgs masses in Table I. QCD background is mainly rejected by a selection requirement on the missing transverse Energy \cancel{E}_T (see Figure 1d) and the scaled missing transverse energy $\cancel{E}_T^{\text{Scaled}}$, which is the \cancel{E}_T divided by the \cancel{E}_T resolution (Figure 2a). This quantity is particularly sensitive to events where the missing energy could be a result of mismeasurements of jet energies in the transverse plane.

$$\cancel{E}_T^{\text{Scaled}} = \frac{\cancel{E}_T}{\sqrt{\sum_{jets} \sigma_{E_T^j}^2 || \cancel{E}_T}}$$

A selection requirement on the minimal transverse mass, M_T^{min} , between one of the leptons and \cancel{E}_T reduces further the various background processes. M_T^{min} at preselection can be found in Figure 2b. The transverse mass is defined as follows:

$$M_T = \sqrt{2 \cdot \cancel{E}_T \cdot p_T^l \cdot (1 - \cos(\Delta\phi))}$$

Remaining $Z/\gamma^* \rightarrow \ell\ell$ events are rejected by requiring the sum of the momentum of $p_T^{e1} + p_T^{e2} + \cancel{E}_T$ to be within a certain mass range as listened in Table I. The $\sum p_T$ distribution on preselection level can be found in Figure 2c. The $t\bar{t}$ contribution is reduced by requiring H_T , the scalar sum of the transverse momenta of all jets in the event, to be lower than 100 GeV. H_T is displayed in Figure 2d at preselection.

After applying cuts 1-6 the remaining background is dominated by electroweak WW and $W + jets/\gamma$ production. At this stage of the selection a Neural Network (NN) is used. The resulting NN output distribution is used for the limit setting procedure. Neural networks are a multivariate technique commonly used in high energy physics. They have been applied in RunI and RunII analysis and are used for b -tagging and object identification techniques ([10], [11]). Neural networks are parameterized nonlinear functions for regression or classification modeling. Inputs to a network are variables that show discrimination between signal and background. Every network used in this analysis consists of three layers of nodes, an input layer, a hidden layer and an output layer. A sigmoid function from the sum of the weighted input variables is calculated at each hidden node. The linear sum of these sigmoid functions appears at the output node. A neural network is trained with samples of simulated signal and background events. During the training process, weights are adjusted at each such that the signal is moved towards one and the background towards zero. The training of the NN has been repeated for each Higgs mass point with WW MC events as background sample and the corresponding Higgs sample as signal input. About 1/3 of the available MC statistics has been used for training purpose. A list of variables sensitive to background and signal has been derived based on the separation power of the various distributions. Those variables can be divided into three classes, object kinematics, event kinematics and angular variables. A detailed list of these variables used for the NN variables can be found in Table II.

These Neural Networks are constructed for each Higgs boson mass point. The NN output for $m_H = 160$ GeV is displayed in Fig. 3.

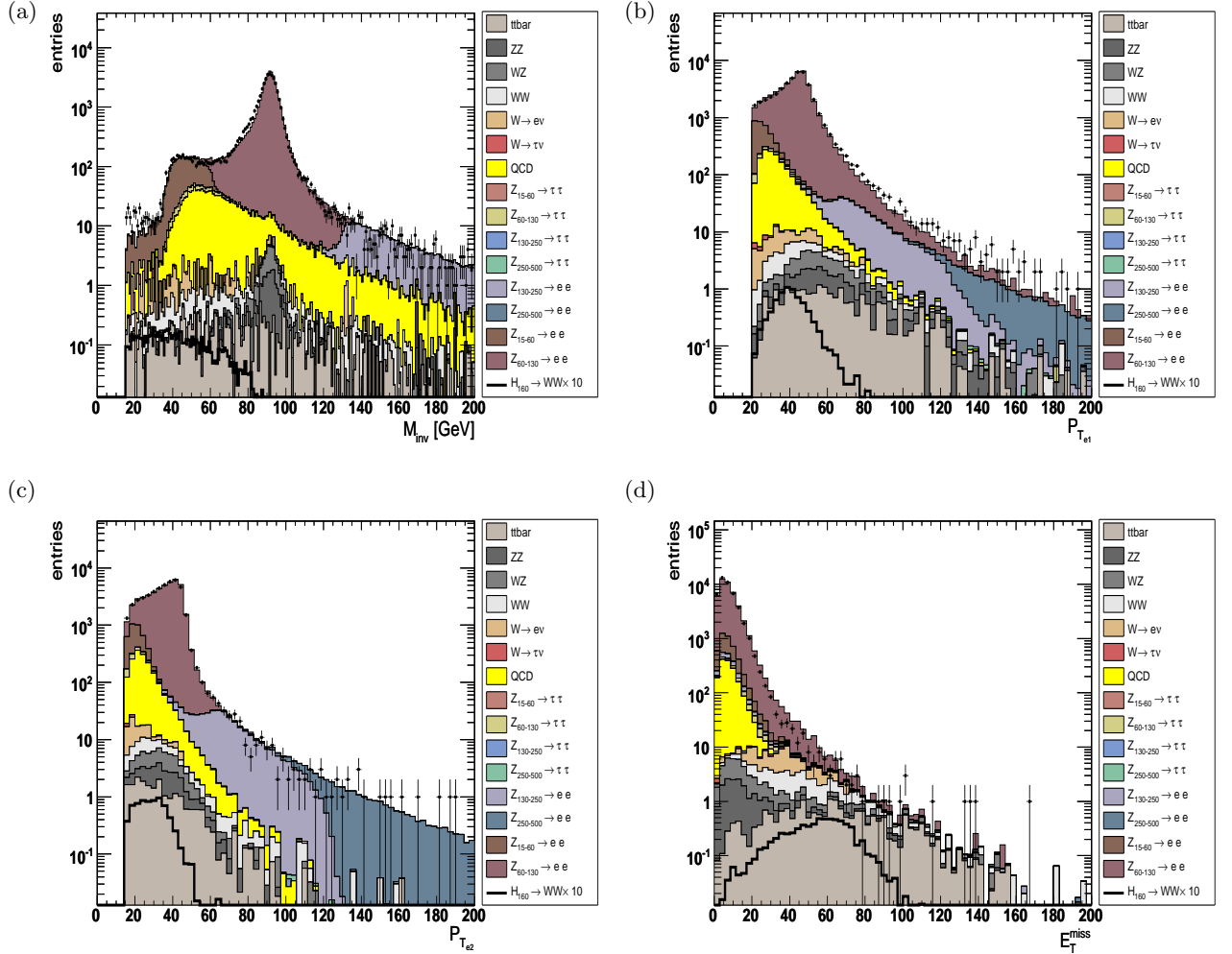


FIG. 1: Distribution of (a) the invariant dilepton mass at preselection level (b) the leading electron p_T at preselection level (b) the next-to-leading electron p_T at preselection level (d) the missing transverse energy, \cancel{E}_T , at preselection level for data (points with error bars), background simulation (histograms, complemented with the QCD expectation) and signal expectation for $m_H = 160$ GeV (empty histogram). The signal contributions for $H \rightarrow WW \rightarrow ee$ are given by the solid line.

IV. SYSTEMATIC UNCERTAINTIES

The estimates for expected numbers of background and signal events depend on numerous measurements that each introduce a systematic uncertainty, lepton identification, trigger efficiencies and reconstruction efficiencies (4%), trigger turn on (4%-7%), jet energy scale calibration in signal ($< 1\%$) and background events (1%), lepton momentum calibration (1%), Parton Distribution Function (PDF) uncertainties ($< 4\%$) and modeling of multijet background (30%). The systematic error on the luminosity is mainly a combination of the PDF uncertainty, uncertainty for the NNLO Z cross section (4%) and data/MC normalization factors (2%). For the estimate of the background remaining after all cuts, the systematic uncertainties are small compared to the statistical uncertainties due to limited MC statistics.

V. RESULTS

Numbers of observed candidates and background events expected after application of the successive selections for $m_H = 120, 140, 160, 180$ and 200 GeV are listed in Tab. III. The total background expectation is dominated by $W + jets/\gamma$ and di-boson events. The number of signal events are in the range of 0.07-0.46 events in the final selection.

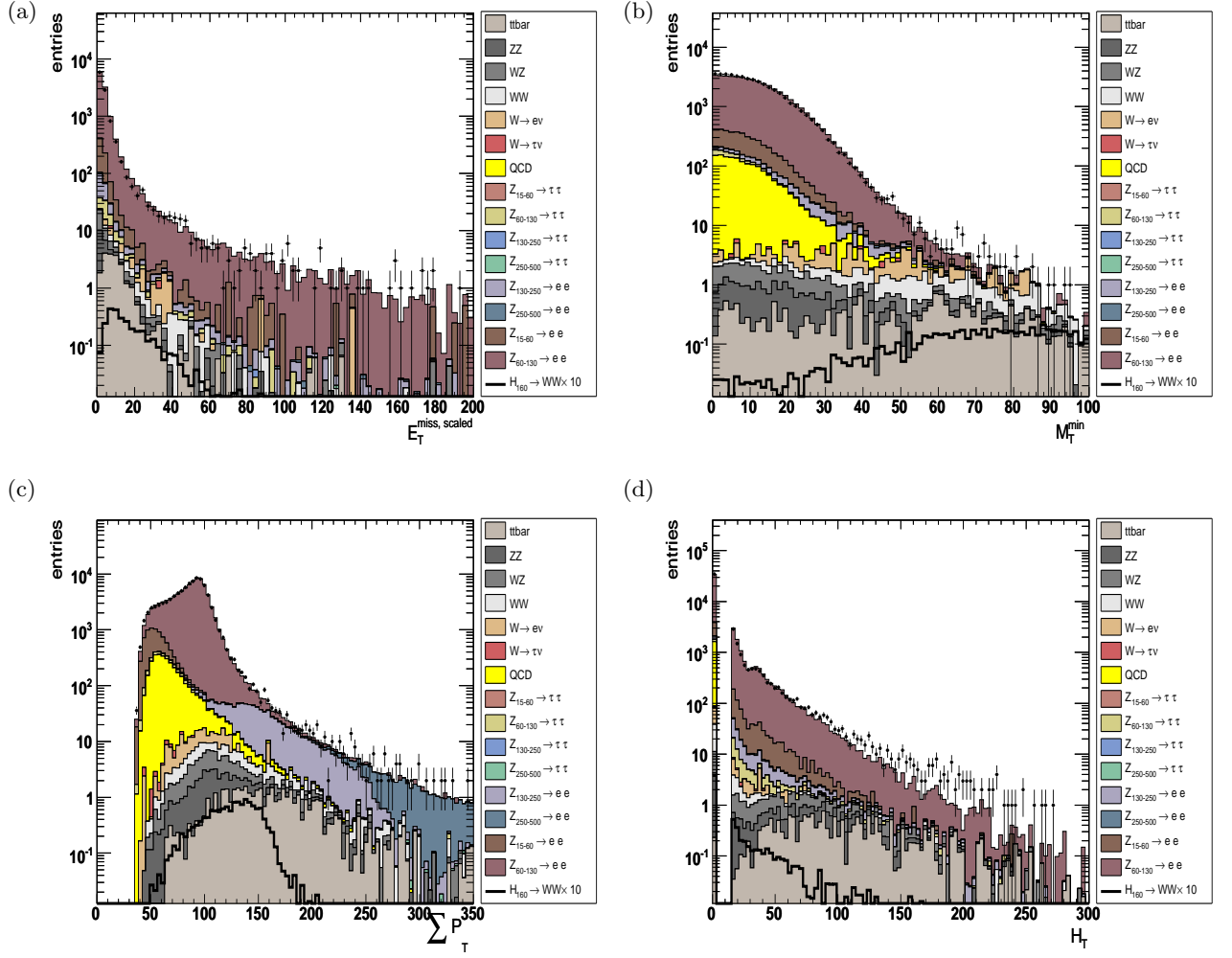


FIG. 2: Distribution of (a) the scaled E_T^{miss} at preselection level (b) the minimal transversal mass M_T^{min} at preselection level (b) the sum of the lepton momentum and E_T , $\sum p_T$, at preselection level (d) the scalar sum of the four leading jet energies, H_T for data (points with error bars), background simulation (histograms, complemented with the QCD expectation) and signal expectation for $m_H = 160$ GeV (empty histogram). The signal contributions for $H \rightarrow WW \rightarrow ee$ are given by the solid line.

NN Analysis Variables	
Object Kinematics	
p_T of leading electron	$p_T(e1)$
p_T of trailing electron	$p_T(e2)$
Event Kinematics	
invariant mass of both leptons	$M_{\text{inv}}(e1, e2)$
minimal transverse mass of one lepton and E_T	M_T^{min}
missing transverse energy	E_T^{miss}
Angular Variables	
angle between selected electrons	$\Delta\phi(e1, e1)$
angle between leading electron and E_T	$\Delta\phi(E_T, e1)$
angle between trailing electron and E_T	$\Delta\phi(E_T, e2)$

TABLE II: Input variables for the Neuronal Network.

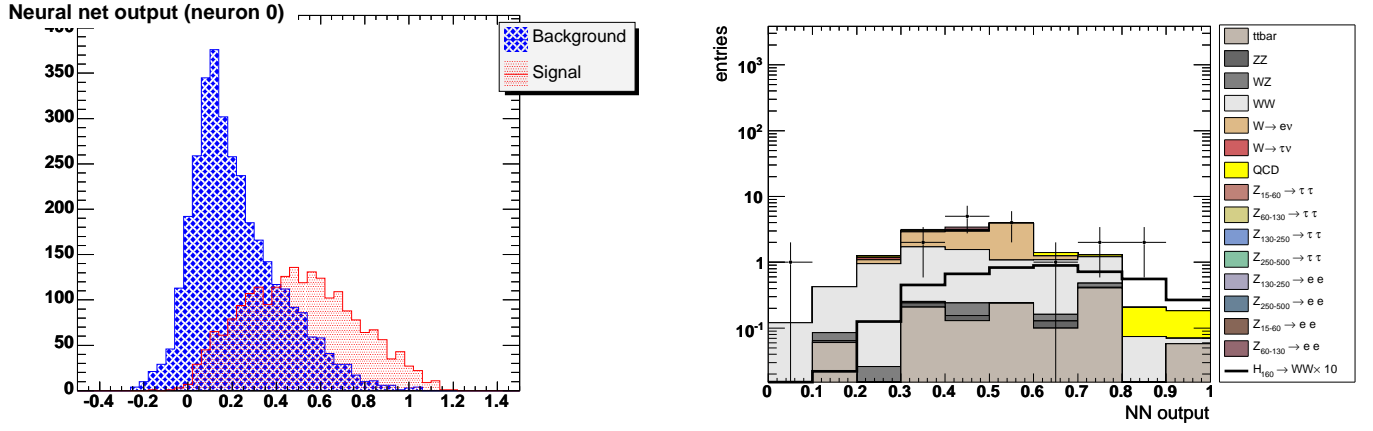


FIG. 3: Neural Network output as results of the training (left) and after applying the last selection requirement as listed in Table I (right). The distributions displayed are with respect to a Higgs mass of $m_H = 160$ GeV. The data is given by points with error bars, the background simulation by filled histograms and the signal expectation by the solid line.

Selection Requirement	Data	Tot. Exp. Bkgd	$H \rightarrow WW$
Preselection $m_H = 120$ GeV	45017.00 ± 212.17	45169.85 ± 101.76	0.14 ± 0.00
Final Selection $m_H = 120$ GeV	21.00 ± 4.58	20.12 ± 2.42	0.07 ± 0.00
Preselection $m_H = 140$ GeV	45017.00 ± 212.17	45169.85 ± 101.76	0.49 ± 0.01
Final Selection $m_H = 140$ GeV	21.00 ± 4.58	21.27 ± 2.26	0.27 ± 0.01
Preselection $m_H = 160$ GeV	45017.00 ± 212.17	45169.85 ± 101.76	0.71 ± 0.01
Final Selection $m_H = 160$ GeV	17.00 ± 4.12	15.49 ± 1.71	0.46 ± 0.01
Preselection $m_H = 180$ GeV	45017.00 ± 212.17	45169.85 ± 101.76	0.53 ± 0.01
Final Selection $m_H = 180$ GeV	17.00 ± 4.12	13.86 ± 1.58	0.28 ± 0.01
Preselection $m_H = 200$ GeV	45017.00 ± 212.17	45169.85 ± 101.76	0.28 ± 0.00
Final Selection $m_H = 200$ GeV	14.00 ± 3.74	10.05 ± 1.33	0.10 ± 0.00

TABLE III: Number of candidate events observed, expected signal and expected background events at different stages of the selection for $m_H = 120, 140, 160, 180$ and $m_H = 200$ GeV. Errors are statistical only

Since after all selection requirements the remaining candidate events are consistent with a background observation, limits on the production cross section times branching ratio $\sigma \times BR(H \rightarrow WW^*)$ are derived following the method described in Ref. [12].

This is done by using the CL_s method with a log-likelihood ratio (LLR) test statistic. This method incorporates systematic uncertainties. Systematics are treated as uncertainties on the expected numbers of signal and background events, not the outcomes of the limit calculations. This approach ensures the the uncertainties and their correlations are propagated to the outcome with their proper weights. The CL_s approach uses binned final-variable distributions rather than a single-bin (fully integrated) value.

Table IV presents the individual observed upper limits on the cross section times branching ratio for the $e^\pm e^\mp$ decay channel and Higgs boson masses $m_H = 120, 140, 160, 180, 200$ GeV. Table V presents the expected limits for the individual channels.

m_H [GeV]	120	140	160	180	200
	observed limit $\sigma \times BR(H \rightarrow WW^* \rightarrow ee)$ [pb]				
ee	12.6	7.4	4.3	5.7	7.6

TABLE IV: Observed upper limits at 95% C.L. on the cross section times branching ratio for $\sigma \times BR(H \rightarrow WW^*)$ for the ee final states.

m_H [GeV]	120	140	160	180	200
	expected limit $\sigma \times BR(H \rightarrow WW^* \rightarrow ee)$ [pb]				
ee	10.1	6.4	2.9	3.2	4.0

TABLE V: Expected upper limits at 95% C.L. on the cross section times branching ratio for $\sigma \times BR(H \rightarrow WW^*)$ for the ee final states.

A graphical representation of the expected and observed limits for the analyzed Higgs boson masses $m_H = 120, 140, 160, 180$ and 200 GeV is displayed in Fig. 4. The expected and observed limits relative to the Standard Model expectation can be found in Figure 5.

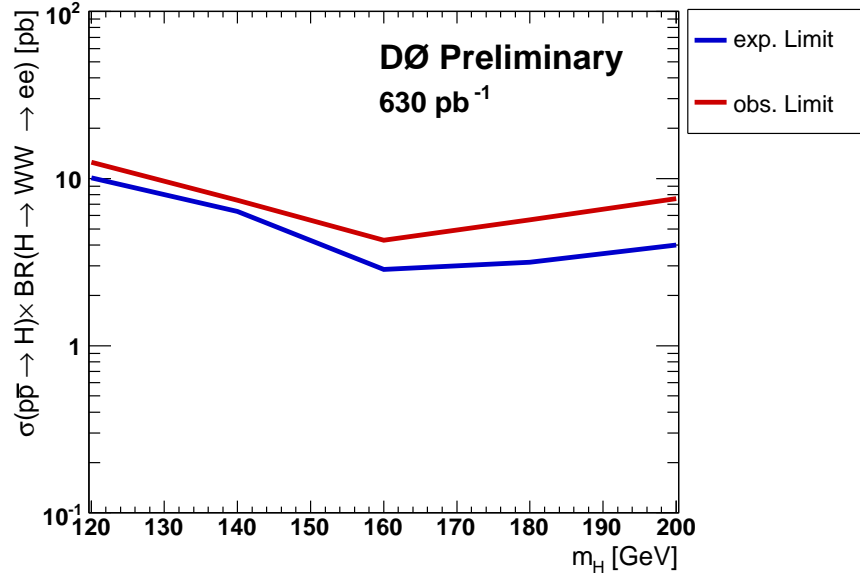


FIG. 4: Expected and observed limits for $m_H = 120, 140, 160, 180$ and 200 GeV. The red line represents the observed limit and the blue one the expected limit.

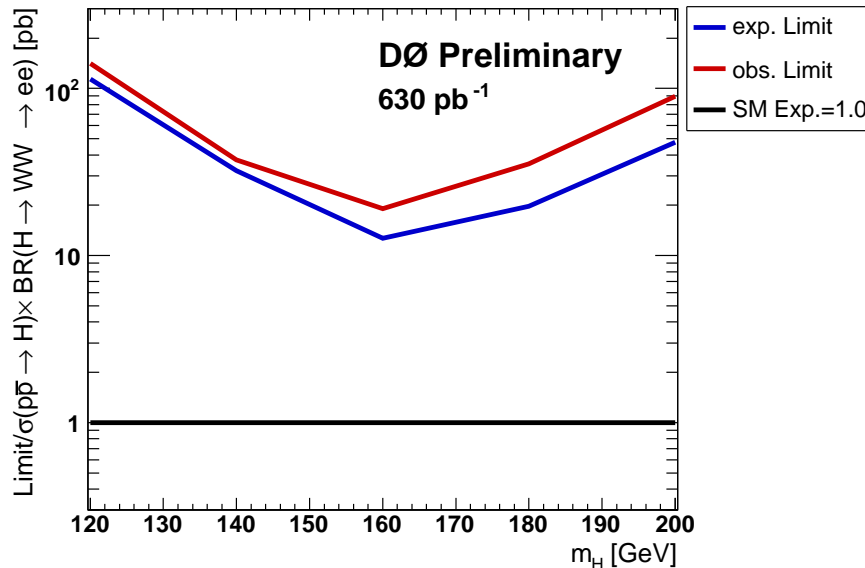


FIG. 5: Expected and observed limits relative to the Standard Model expectation for $m_H = 120, 140, 160, 180$ and 200 GeV. The red line represents the observed limit and the blue one the expected limit. The Standard Model expectation is given by the solid black line.

VI. CONCLUSIONS

A search has been performed for the $H \rightarrow WW \rightarrow \ell\ell$ decay signature of the Standard Model Higgs boson in leptonic channels with two electrons, using data corresponding to an integrated luminosity of 630 pb^{-1} . No evidence for the Higgs particle is observed and upper limits using this channel on the product of cross section times branching ratio are set. Combined with existing $H \rightarrow WW \rightarrow \ell\ell$ analysis previous limits can be improved.

Acknowledgments

We thank the staffs at Fermilab and collaborating institutions, and acknowledge support from the Department of Energy and National Science Foundation (USA), Commissariat à l’Energie Atomique and CNRS/Institut National de Physique Nucléaire et de Physique des Particules (France), Ministry of Education and Science, Agency for Atomic Energy and RF President Grants Program (Russia), CAPES, CNPq, FAPERJ, FAPESP and FUNDUNESP (Brazil), Departments of Atomic Energy and Science and Technology (India), Colciencias (Colombia), CONACyT (Mexico), KRF (Korea), CONICET and UBACyT (Argentina), The Foundation for Fundamental Research on Matter (The Netherlands), PPARC (United Kingdom), Ministry of Education (Czech Republic), Natural Sciences and Engineering Research Council and WestGrid Project (Canada), BMBF (Germany), A.P. Sloan Foundation, Civilian Research and Development Foundation, Research Corporation, Texas Advanced Research Program, and the Alexander von Humboldt Foundation.

-
- [1] T. Hao, A. Turcot, R.-J. Yang, Phys. Rev. D. **59**, 093001 (1999).
 - [2] M. Carena *et al.* [Higgs Working Group Collaboration], “Report of the Tevatron Higgs working group”, hep-ph/0010338.
 - [3] K. Jakobs, W. Walkowiak, ATLAS Physics Note, ATL-PHYS-2000-019.
 - [4] M. Titov, D0 Note 005063, “Search for the Higgs boson in $H \rightarrow WW \rightarrow l^+l^- (ee, e\mu)$ decays with 950 pb^{-1} at D0 in Run II”
 - [5] T. Sjöstrand, Comp. Phys. Commun. **82** (1994) 74, CERN-TH 7112/93 (1993).
 - [6] A. Djouadi *et al.*, Comput. Phys. Commun. **108**, 56 (1998).
 - [7] R. Hamberg, W.L. van Neerven, and T. Matsuura, Nucl. Phys. **B359**, 343 (1991) [Erratum-ibid. **B644**, 403 (2002)].
 - [8] T. Nunnemann, D0 Note 4476.
 - [9] N. Kidonakis, R. Vogt, hep-ph/0410367, published in Int.J.Mod.Phys.A20:3171, 2005.

- [10] DØ note 5228, “Using Bayesian Neural Networks to Search for Single Top Quarks in 1fb^{-1} of Data”.
- [11] DØ note 5094, “ τ identification with neural networks for $p17$ data”.
- [12] T. Junk, Nucl. Instr. and Meth., A434(1999) 435